Science in China Series D: Earth Sciences

www.scichina.com
earth.scichina.com
www.springerlink.com

The uplifting process of the Bogda Mountain during the Cenozoic and its tectonic implication

WANG ZongXiu[1], LI Tao[2], ZHANG Jin[2] , LIU YongQing[3] & MA ZongJin[2]

[1] Institute of Geomechanics, Chinese Academy of Geological Sciences, Beijing 100081, China;
[2] Institute of Geology, China Seismological Administration, Beijing 100029, China;
[3] Institute of Geology, Chinese Academy of Geological Sciences, Beijing 100037, China

The Tianshan Mountains have undergone its initial orogeny, extension adjusting and re-orogeny since the Late Paleozoic. The re-orogeny and uplifting process of the orogeny in the Mesozoic and Cenozoic are two of most important events in the geological evolution of Euro-Asian continent, which resulted in the formation of the present range-and-basin pattern in topography of the Tianshan Mountains and its adjacent areas. Thermochronology results by the method of fission-track dating of apatite suggest three obvious uplifting stages of the Bogad Mountain Chain re-orogeny during the Cenozoic, i.e. 5.6—19 Ma, 20—30 Ma, and 42—47 Ma. The strongest uplifting stage of the mountain is the second one at 20—30 Ma, when the mountain uplifted as a whole, and the beginning of re-orogeny was no less than 65 Ma. Furthermore, our studies also show that the uplifting types of the mountain are variable in the different time periods, including uplifting of mountain as a whole and differential uplifting. The apparently diversified uplifting processes of the mountain chain are characterized by the migration (or transformation) of the uplifting direction of the mountain from west to east and from north to south, and the main process of mountain extending is from north to south.

Bogda Mountain Chain, re-orogeny, uplifting, thermochronology, fission track

1 Introduction

The Tianshan Mountains, located in the middle Eurasia, is a great mountain chain, which underwent long-term and complicated evolution. More attention has recently been paid to this great mountain on different aspects[1−4]. Studies have showed that the Cenozoic uplifting of the Tianshan Mountains resulted from the intraplate crust shortening[5], the thrust faults and related folds developed in and along the boundaries of the mountain. There have been many studies and related references about the uplifting of the Tianshan Mountains, but most of scattered data come from southwest and northern Tianshan Mountains, and complete and accurate chronological data from the eastern Tianshan Mountains are lacking. Fission track dating method of apatite reveled the uplifting ages of the southwestern Tianshan Mountains varying from 134 Ma to 109 Ma by Yang et al.[6], northern Tianshan Mountains at 89 Ma by Wang et al.[7], and southern Tianshan Mountains ranging from 109 Ma to 68 Ma by Zhou et al.[8] and Gong et al.[9], respectively. In the eastern Tianshan Mountains (the Bogda Mountian), the thermochronological data of uplifting of mountain are even fewer because of the lack of intrusions that can be effectively used for dating. Fission track dating analysis results by Hendrix et al.[1] showed the unroofing of the northern Tianshan Mountains varying from later Oligocene to early Miocene, that is to say that the Tianshan Mountains uplifted 24 Ma ago. Windley et al.[10] and Allen et al.[11] pointed out that the

Received September 14, 2007; accepted January 18, 2008
doi: 10.1007/s11430-008-0038-z
†Corresponding author (email: wangzongxiu@sohu.com)
Supported by the National Basic Research Program of China (973 Program)(Grant No. 2007CB411305), National Science Foundation of China (Grant No. 40572116) and National Project of Geological Survey (Grant No. 200113000078)

angle unconformity between Oligocene molasses with lower strata in Eastern Tianshan Mountains implied the beginning time of the uplifting of Tianshan Mountains. Based on the distribution of Cenozoic strata, Deng et al.[4] conjectured that the uplifting of the Tianshan Mountains might begin at the early Miocene. To sum up, the uplifting characteristics and process of the Tianshan Mountains during the Cenozoic are not clear yet because of lack of samples and systematic sampling along trans-sections cross the mountain. Therefore, systematic research on the beginning time and uplifting stages of the great eastern Tianshan-Bogda mountain chain (including the Bogda Mountain and the Balikun Mountain) were carried out based on the fission track thermochronological dating method of apatite.

2 Geological setting

The Bogda and Balikun Mountains was once called as the eastern Tianshan Mountains in Chinese literature, which is located to the north of the Turpan-Hami Basin and to the south of eastern Junggar Basin. The mountain chain is mainly composed of Carboniferous and Permian clastic rocks and some mafic intrusions. The whole mountain mainly strikes east–west and about 360 km long, 40—60 km wide (Figure 1). Some workers thought that the mountain was one island-arc during the Late Paleozoic[12,13], but the others argued it was once a rift or aulacogen[14]. Recent studies have shown the Bogda Mountain chain had undergone initial orogeny during 310—316 Ma[15]. In the Mesozoic the mountain chain had extended, and the Jurassic strata with coal mine had deposited across the mountain, which means that the mountain had already been denudated. During the Cenozoic, the mountain has undergone strong uplifting because of strike-slipping or the Indo–Eurasian collision[16].

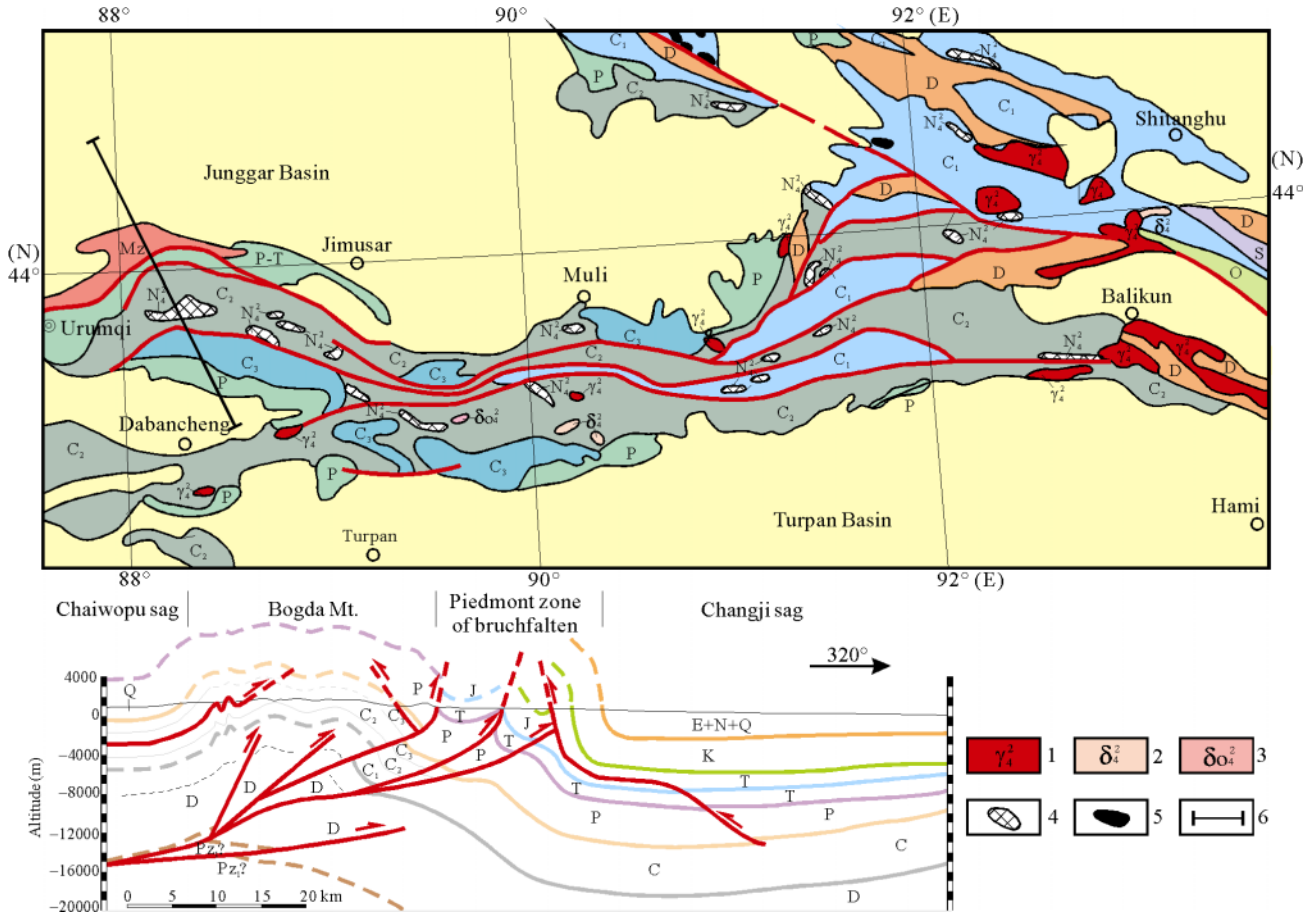

Figure 1 Generalized geological map of Bogda Mountain and its adjacent area. 1, Hercynian granite; 2, Hercynian diorite; 3, Hercynian quartz diorite; 4, Hercynian basite; 5, ophiolite; 6, profile place.

3 Burying of the mountain and change of the Paleo-geothermal gradient

3.1 Burying of the mountain

Studies have showed that the Bogda Mountain had undergone initial orogeny in Late Paleozoic (310—316 Ma), extension adjusting in Mesozoic and re-orogeny in the Cenozoic[1)]. In the whole Mesozoic, the Junggar Basin, the Turpan-Hami Basin and the Tarim Basin underwent pan-lake sedimentation for several times, and these three basins may have linked with many small intermontane basins in the Tianshan Mountains[17]. In addition, the following facts also suggested that the Bogda mountain formed during the Late Paleozoic had been eroded and buried by Mesozoic sediments: 1) the Mesozoic sediments since the Late Triassic to the north and south of the mountain can be well compared, and no rejuvenated foreland basin developed; 2) the Mesozoic strata along the two sides of the Bogda Mountain become finer upwards as a whole, and the components trend more mature gradually, which showed that the high rate between paleo-Bogda mountain and basins became smaller and smaller; 3) in the Tangfang valley (2000 m above the sea level) in the Bogda Mountain, the remnant Middle-Lower Jurassic coal-bearing strata were found, these fluvial, lake and swamp sediments mean that during that time the mountain had already been eroded; 4) these strata are the newest strata preserved before the Cenozoic uplifting, and furthermore, its diagenesis degree , coal and coal rank(flame coal) are similar to the same strata in the foreland regions, which means that the paleo-Bogda Mountain was buried deeply and underwent deep buried metamorphism at least since the Jurassic; 5) in the Cretaceous, basins along the two sides of the Tianshan Mountains once again underwent pan-lake sedimentation, the Cretaceous strata overlapped marginal uplifts and mountains widely[17], with phenomena mentioned in 4); we conjecture that the Bogda Mountain region had already eroded down, and began to receive sediments. The above discussions indicate that the Paleozoic and Triassic strata in the Bogda region were buried deeply because of the covering of the Jurassic-Cretaceous and Paleogene systems, based on regional data of these three systems, we conjecture that the surface of the Bogda Mountain was buried at least for 3000 m deep. Therefore, the outcropped Carboniferous strata which comprised the present mountain resulted neither from thrusting or gravity sliding, nor from non-sedimentation since the Late Paleozoic, but from the unroofing since the Cenozoic.

3.2 Change of the paleo-geothermal gradient

After the Late Paleozoic, the tectonic movement in the Tianshan Mountains and the basins along two sides became weaker or even dormant, no magmatism and volcanism had occurred here since Late Permian The paleo-geothermal gradient became smaller gradually, and the Tarim Basin, the Junggar Basin and the Turpan-Hami basin all underwent similar process. Based on the inversion of the organic matter maturity R_0 in basins adjacent to the mountain, we obtain the paleo-geothermal data (Table 1, Figure 2), and these data showed that the paleo-geothermal gradient of the eastern Junggar Basin declined continuously from the Late Carboniferous to the Neogene, and the starting point of the paleo-geothermal gradient in the northeastern Junggar Basin (foreland region of the Kelameili Mountain) was lower and declined with low slope However, the starting point in the foreland of the Bogda Mountain was much higher and declined much rapidly, which resulted in the same gradient as that in the northeast part of the Junggar Basin during the Late Permian, and in the Paleogene it was smaller than one in the northeastern basin. The paleo-geothermal data in the foreland region of the Bogda Mountain make up of three "flats" (Figure 2), which are Early–Middle Permian, Late Permian–Late Cretaceous and after Paleogene, respectively. These three flats correspond well to the three tectonic stages of the Bogda Mountain since the Late Paleozoic. The magmatism and volcanism in the Bogda Mountain and adjacent basins did not occur since the Late Permian; the change of sediment rate also showed the weakening of tectonic movement (Figure 3). Therefore, we suggest that the Bogda region underwent continuous heat attenuation from the Late Paleozoic on, and the thermal depression after the rifting stage was the main characteristics in this region in the Mesozoic. Because the evolution of basins were controlled or affected by the marginal mountains in

1) Wang Z X. Orogeny, formation and evolution of Bogad Mountain, Northwest China. Dissertation for Doctoral Degree. Beijing: Institute of Geology, China Seismological Administration, 2003. 30—55

the studied region, the change of the paleo-geothermal gradient of basins may indicate the tectonic history of the adjacent mountain indirectly.

Table 1 Paleo-geothermal gradient of the eastern Junggar Basin

Geological time	Paleo-geothermal gradient (℃/100 m)	
	Northeastern Junggar Basin	Foreland of the Bogda Mountain
Late Carboniferous	4.11	
Early Permian	3.95	5.3
Middle Permian	3.5	5.2
Late Permian	3.44	3.5
Triassic	3.44	3.5
Jurassic	3.15	3.5
Cretaceous	3.15	3.5
Paleogene	2.65	2.42
Neogene	2.65	2.42

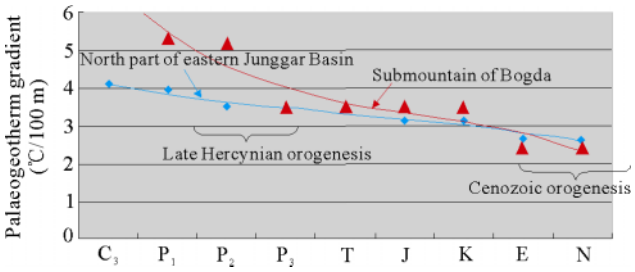

Figure 2 Evolution curve of the paleo-geothermal gradient of the eastern Junggar Basin.

The present geotemperature distribution vs. depth from the regions around the eastern Junggar Basin showed that the geotemperature became more linear with the deepening (Figure 4). Based on the present surface temperature (20℃) and the above-measured geothermal data, the geotemperature vs. depth formula is best fitted:

$$Y=26.757X-414.19,$$

in which X is the temperature, Y is the depth.

Based on this formula, the temperature has already been 110—120℃ in 3000 m deep, and the apatite has been annealed. We know from those mentioned above that the geotemperature of eastern Junggar Basin has declined continuously, so in the same depth, the apatite was also annealed completely.

4 Sampling

4.1 Rules of sampling

First, in the study of the mountain uplifting, the ideal samples for fission track dating are basement rocks of mountains, such as granite which emplaced during one thermal event as single intrusive body, during late uplifting, the rocks underwent unroofing to arrive at the earth surface, for these rocks could record the information of fission track ages during the cooling process. However, in many studies, due to different conditions, the above constrains for sampling could not be satisfied. Second, in many studies of the fission track dating in mountain uplifting, data from one or several profiles were used to depict the uplifting process of the whole mountain. We argue that tectonic segmentation was one of basin characteristics of the mountain uplifting, and different segments have their own uplifting processes. Hence one or two profiles could not delineate the general uplifting process of the whole mountain, furthermore, the uplifting of two slopes of mountains are even different, which may result in more complex uplifting style. Therefore, in addition to the sampling along different profiles, regional sampling of the mountain is needed. In the Bogda-Balikun Mountains there are neither large scale granite nor single rock body of certain scale with enough height difference. So in order to avoid deviations due to the routine sampling, we sampled in different structural parts of the whole mountain, and massive and systematic sampling were carried out for apatite fission track dating in the Carboniferous-Permian System, the Triassic System and intermediate and basic intrusive bodies.

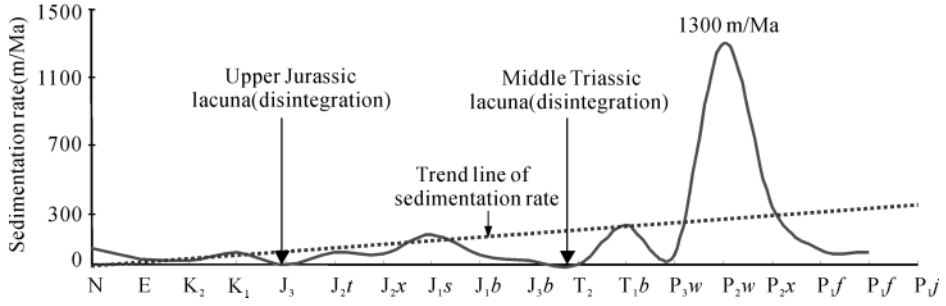

Figure 3 Sediment curves of different strata of the Junggar Basin.

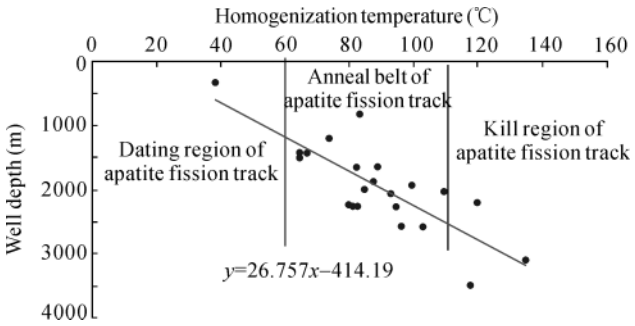

Figure 4 Distribution of temperature vs. depth in the regions around the eastern Junggar Basin (temperature was measured by inclusions obtained in wells). (Data from Petroleum University at Dongying, 2000).

4.2 Distribution of the samples

The low thermochronological dating of the Cenozoic uplifting of the Bogda-Balikun Mountains is based on the many successful studies on the deformation styles, uplifting mechanism and segmentation of these mountains. Therefore, the sampling and dating in this study not only have unambiguous intentions but also were controlled well on the regional scale. The sample locations were showed in Figure 5. As showed in Figure 5, the sample points covered the Bogda-Balikun Mountains. Among them, parts of samples were collected along two north-south trending sections across the mountain (Mulei-Gaoquandaban-northern Turpan-Hami Basin section to the west and Qijiaojing-Dashitou section to the east), and the rest samples were collected in the northern and southern foothills of the mountain to compare the uplifting of the mountain across the strike and discuss the deformation style Moreover, in order to compare the uplifting of the mountain along the strike, we collected the samples along the whole mountain chain. At last, in order to compare the sequence of the uplifting of the two slopes due to the southward undertrusting of the basement of the Changji Basin and discuss the kinematical vergence and symmetry of the two limbs of the Bogda Mountain box anticlinorium during the deformation, samples were also collected symmetrically in the two slopes of the mountain. In the following analysis, the study divided the whole mountain into two segments taking the north–south section passing Qijiaojing as the boundary; and in order to focus the Bogda Mountain, the study also divided the mountain into two parts taking the watershed of the mountain as the boundary.

5 Thermochronological analysis

5.1 Experiment conditions and testing process

Apatite fission track ages were obtained using the external detector method[18] and calculated by the zeta calibration method[19]. Age-calibration standard is Durango apatite (31.4 Ma). The National Bureau of Standards trace element glass SRM_{612} was used as a dosimeter to measure the neutron fluencies during irradiation.

Spontaneous fission tracks in apatite were etched in 7%HNO_3 at 20℃ for 35 s. Induced fission tracks in the low-U muscovite external detectors that covered apatite grain mounts and glass dosimeters during the irradiation were later etched in 40%HF at 20℃ for 20 min.

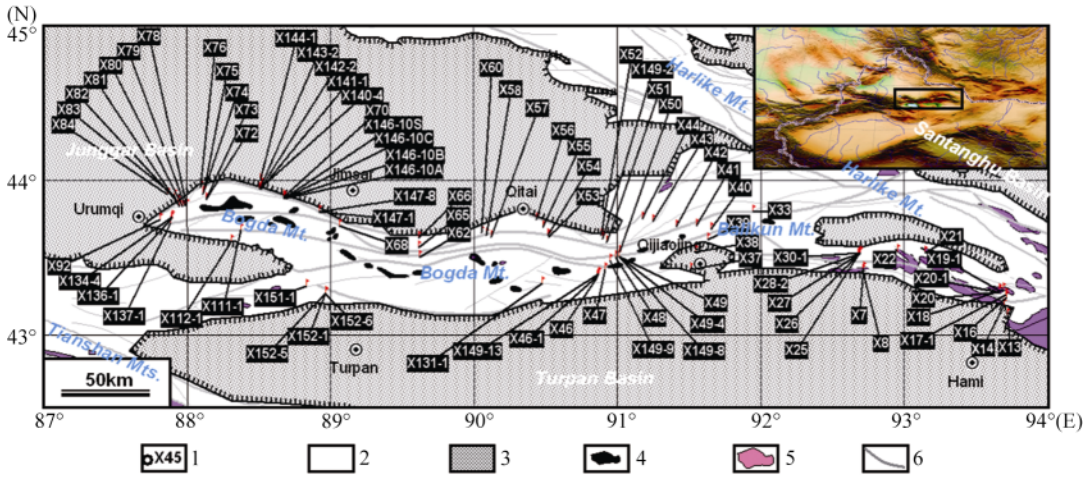

Figure 5 Distribution of samples and Position of study area. 1, Location of sampling; 2, mountain; 3, basin; 4, intrusive body; 5, granite; 6, fault.

Fission tracks and track–length measurements were counted on an OLYMPUS microscope, using a magnification of 1000 under oil immersion objectives for apatite.

All analyses were performed in the State Key Laboratory of Seismic Dynamics in Institute of Geology, China Seismological Administration. A total of 72 effective apatite samples and 9 zircon samples for fission track dating were obtained.

5.2 Data analysis

Table 2 showed the measured fission track data of the Bogda-Balikun Mountain In Table 2 the $P(x^2)$ is the probability where degrees of freedom=$(n^{-1})x^2$, and can be calculated by N_i and N_s in the table. When $P(x^2)$ >5%, the ages of samples are composite ages; when $P(x^2) \leqslant 5\%$, the ages of samples are mean ages. Error is marked by $\pm 1\sigma$, and the σ can be obtained by above formula. The implications of other parameters in Table 2 were noted at the end of the table.

The data in Table 2 show that the apatite fission track ages of the Bogda-Balikun Mountains range from 5.6 to 65.6 Ma.

Because the fission tracks in the mineral were formed in different periods, so the length distribution is the basic reflection of the heating history of the mineral. If the fission tracks were completely closed in the mineral after etching, then this kind of track is called confined track. The length of confined track is equal to the recorded range of spontaneous fission fragments of ^{238}U in the mineral. The change of recorded ranges according to the temperature is the important marker of the annealing process, so the length distribution of the confined track is true reflection of the thermal history of the mineral.

The measured lengths of fission tracks were showed in Figure 6. Compared with the apatite length distributions of different kinds of thermal histories[18], the apatite fission track type of the Bogda-Balikun Mountains mainly belongs to the type of non-disturbance basement, which indicates that the thermal history of the Cenozoic uplifting of the mountain was much simpler generally, i.e. the mountain did not undergo heating again during the cooling process Some samples showed annealing phenomenon with the peak of short tracks, which may have resulted from burying for not deep enough in local regions. The length style of the apatite fission track of the Bogda-Balikun Mountains indicates that the studied region underwent continuously heat attenuation since the Late Paleozoic, and the strong tectonic event occurring in southwest Tianshan Mountains in the Triassic-Jurassic was not recorded in the studied region.

Because of no further annealing events, the fission tracks developing by cooling after the thermal event did not shorten, and therefore, what they recorded was the information of the unroofing of the mountain. And the length distribution of the tracks was controlled by the thermal history of the rocks so constrained by the facts of temperature and age; one fitted curve of the changes of the uplifting rate could be obtained.

Analysis results of fission-track dating of apatite are listed in Table 2.

In order to obtain the characteristics of distribution of 43 fission track ages, the data are re-ordered to better show the whole distribution of cooling age of the mountain chain. The results revealed the fission track ages of apatite ranging from 65.5 to 5.6 Ma, there are three main more-concentrated periods, i.e. 5.6－19 Ma, 20－30 Ma and 42－47 Ma (Figure 7), and the medians of these three periods are 13.0, 24.4and 45.4 Ma, respec tively.

6 Uplifting rate and cooling pattern

6.1 The age of initial uplifting and main uplifting period

Based on the distribution of fission–track age (Figures 7 and 8), the fission track ages of apatite in studied region range from 5.6 to 65.6 Ma, and the distribution of these ages (Figure 8) showed the uplifting characteristics of the whole mountain. Just as those mentioned above, the uplifting of the mountain can be divided into early slow uplifting and late rapid one, and this phenomenon can be also found in the distribution of the fission track ages.

The fission track ages of the apatite of the studied region show that the initial uplifting of the Bogda-Balikun Mountains in the Cenozoic began at 65.6 Ma (Figure 8); however the samples of this period only are 10% of all samples, and most of them were sampled from the western part of the Bogda mountain, which indicates that the initial uplifting did not occur across the whole mountain. The main uplifting period is 15.6－25.6 Ma (Figure 8) when the whole mountain began to undergo uplifting for the first time.

Table 2 The fission track data of Bogda–Balikun Mountains (apatite)[a)]

Lab No.	Sample No.	Altitude (m)	N_c	$\rho_d(N_d)$ ($\times10^6$ cm^{-2})	$\rho_s(N_s)$ ($\times10^5$ cm^{-2})	$\rho_i(N_i)$ ($\times10^6$ cm^{-2})	U concentration (ppm)	$P(x^2)$ (%)	r	Fission track age±1σ (Ma)	Mean track length±1σ (μm) (N_j)	Standard deviation (μm)
L1	X7	2040	7	1.159(2885)	0.8378(31)	0.9243(342)	9.8	99.30	0.977	18.5±3.8	13.11±0.48(10)	1.520
L2	X8	1980	22	1.165(2900)	1.651(199)	1.524(1873)	16.1	98.50	0.942	22.2±2.5	13.00±0.18(52)	1.340
L3	X13	1488	22	1.171(2915)	0.6188(87)	1.038(1460)	10.9	1.0	0.567	15.1±2.2	12.88±0.41(16)	1.640
L4	X14	1783	10	1.176(2930)	0.5473(22)	1.455(585)	15.2	59.0	0.649	7.8±1.8	12.32±1.29(3)	2.240
L6	X16	2215	22	1.188(2960)	2.239(244)	1.529(1667)	15.8	0.843	0.892	28.2±2.9	13.46±0.26(35)	1.560
L7	X17-1	2433	3	1.194(2975)	3.900(117)	2.487(746)	25.6	12.4	0.922	32.9±4.3	13.17±0.36(15)	1.390
L8	X18	2737	35	1.200(2990)	0.1222(22)	0.4589(826)	4.7	21.6	0.352	5.6±1.3	10.72±1.29(2)	1.830
L9	X19-1	3213	22	1.206(3005)	1.173(115)	0.9102(892)	9.3	100	0.899	27.3±3.6	13.30±0.17(63)	1.410
L10	X20	3254	22	1.212(3020)	0.8643(121)	0.7500(1050)	7.6	97.5	0.925	24.6±3.1	13.75±1.16(5)	2.600
L11	X20-1	3254	22	1.218(3035)	0.7850(168)	0.7206(1542)	7.3	100	0.926	23.3±2.7	14.52±0.21(18)	0.900
L12	X21	2212	22	1.224(3050)	0.500(35)	0.8186(573)	8.3	99.5	0.891	13.2±2.5	12.74±0.26(4)	0.530
L13	X22	2205	22	1.230(3065)	1.353(188)	1.214(1687)	12.1	99.4	0.922	24.1±2.7	13.24±0.17(58)	1.350
L14	X25	2810	15	1.236(3080)	0.6774(42)	0.7516(466)	7.5	99.9	0.943	19.6±3.6	14.02±0.47(11)	1.580
L15	X26	2616	22	1.241(3095)	0.6386()	0.9918(848)	9.8	62.0	0.590	14.1±2.3	12.79±0.31(18)	1.350
L16	X27	2470	22	1.247(3110)	1.288(134)	1.741(1181)	17.2	47.7	0.845	16.2±2.0	12.06±0.36(27)	1.880
L17	X28-2	2352	9	1.253(3125)	0.6897(20)	0.8862(257)	8.7	90.1	0.983	17.2±4.2	12.19±0.33(9)	1.000
L18	X30-1	2174	10	1.259(3140)	0.8525(52)	0.9689(1776)	9.5	31.1	0.813	19.5±3.3	12.99±0.37(11)	1.230
L19	X33	2001	22	1,265(3255)	1.233(148)	1.154(1385)	11.2	46.9	0.965	23.8±2.9	12.68±0.24(24)	1.200
L20	X37	953	22	1.271(3170)	0.6731(70)	0.7019(730)	6.8	100	0.878	21.4±2.1	12.29±0.27(16)	1.080
L21	X38	944	22	1.277(3185)	0.4432(39)	1.035(911)	10.0	4.7	0.598	10.5±2.1	12.32±0.31(10)	0.990
L22	X39	1129	22	1.283(3200)	0.9278(90)	0.8732(847)	8.4	99.3	0.969	24.0±3.3	12.43±0.49(33)	2.860
L25	X42	1686	19	1.300(3245)	0.6901(49)	0.7028(499)	6.6	81.1	0.960	22.5±3.9	12.61±0.45(5)	1.010
L26	X43	1486	16	1.306(3260)	0.9452(69)	0.9055(661)	8.5	69.1	0.827	24.0±3.6	13.26±0.00(1)	0.000
L27	X44	1399	22	1.312(3275)	2.761(323)	1.126(1318)	10.6	0.0	0.805	45.7±8.7	13.53±0.27(30)	1.520
L28	X46	1504	13	1.318(3290)	1.368(78)	1.440(821)	13.4	79.9	0.957	22.0±3.2	14.34±0.36(17)	1.500
L29	X46-1	1504	22	1.324(3305)	1.375(150)	1.511(1648)	14.0	0.034	0.868	19.6±3.0	13.49±0.34(23)	1.660
L31	X48	2017	22	1.336(3335)	0.9785(114)	1.327(1546)`	12.2	35.2	0.881	17.3±2.2	14.13±0.19(42)	1.270
L32	X49	2198	6	1.342(3350)	0.5758(19)	0.6121(202)	5.6	10.9	0.421	22.2±5.6	13.68±0.26(16)	1.060
L33	X49-4	2198	5	1.348(3365)	0.4737(9)	0.4895(93)	4.5	25.4	0.134	22.9±8.2	11.06±0.38(4)	0.760
L34	X50	1906	5	1.354(3380)	0.7778(14)	0.6278(113)	5.7	96.6	0.888	29.5±8.7	12.05±1.29(2)	1.830
L35	X51	1716	15	1.359(3395)	0.5828(38)	0.5031(328)	4.6	94.2	0.858	27.7±5.3	14.09±0.28(18)	1.190
L36	X52	1597	22	1.365(3415)	2.411(258)	1.959(2096)	17.6	99.7	0.993	29.5±3.2	13.99±0.2(52)	1.510
L39	X55	1654	22	1.383(3455)	1.422(293)	0.5279(1088)	4.7	92.7	0.983	65.3±7.0	13.61±0.21(26)	1.110
L40	X56	1488	15	1.389(3470)	2.389(215)	1.282(1154)	11.4	41.9	0.962	45.4±5.1	13.35±0.20(32)	1.260
L42	X58	1718	14	1.395(3485)	1.092(83)	0.6013(457)	5.3	46.0	0.816	44.5±6.5	13.26±0.49(14)	1.830
L43	X60	1537	22	1.401(3500)	0.687(79)	0.5887(677)	5.2	89.2	0.797	28.7±4.2	13.30±0.28(25)	1.430
L44	X62	2200	4	1.407(3515)	2.211(21)	1.179(112)	10.3	99.9	1.000	46.3±11.7	12.65±1.42(3)	2.470
L50	X73	1908	22	1.182(2945)	1.246(129)	1.135(1175)	11.8	100.0	0.957	22.8±2.9	12.80±0.21(53)	1.530
L53	X76	1280	22	1.199(3012)	0.8434(83)	0.6453(635)	6.6	41.1	0.816	27.6±4.0	14.65±0.27(19)	1.180

(*To be continued on the next page*)

(*Continued*)

Lab No.	Sample No.	Altitude (m)	N_c	$\rho_d(N_d)$ ($\times10^6$ cm^{-2})	$\rho_s(N_s)$ ($\times10^5$ cm^{-2})	$\rho_i(N_i)$ ($\times10^6$ cm^{-2})	U concentration (ppm)	$P(x^2)$ (%)	r	Fission track age±1σ (Ma)	Mean track length±1σ (μm) (N_j)	Standard deviation (μm)
L54	X78	2081	22	1.188(2983)	0.8677(62)	1.553(1118)	16.1	29.3	0.826	11.6±1.8	13.52±0.42(9)	1.270
L55	X79	1856	6	1.177(2954)	0.6429(9)	0.6929(97)	7.2	79.9	0.557	19.2±6.9	14.35±0.00(1)	0.000
L56	X80	1679	14	1.166(2925)	0.4262(26)	0.5557(339)	5.9	86.2	0.385	15.7±3.5	12.10±0.32(2)	0.450
L57	X81	1501	16	1.155(2896)	0.4037(22)	0.5505(300)	5.9	62.4	0.560	14.9±3.5	14.35±0.00(1)	0.000
L60	X84	970	22	1.122(2809)	1.379(142)	0.8049(829)	8.8	94.2	0.885	33.8±4.2	13.79±0.19(49)	1.370
L62	X68	1841	22	1.100(2751)	0.5909(65)	0.4891(538)	5.5	100.0	0.924	23.4±3.6	12.76±0.51(8)	1.460
LT1	X146-10A	2094	6	1.338(3349)	5.014(178)	1.335(474)	12.3	19.0	0.979	87.9±10.7	13.36±0.31(16)	1.240
LT2	X147-1	1890	21	1.344(3363)	5.107(549)	1.497(1609)	13.7	0.000	0.968	47.6±8.2	13.80±0.19(67)	1.610
LT3	X147-8	1890	21	1.353(3384)	2.924(333)	0.6514(742)	5.9	0.000	0.930	57.4±11.1	12.78±0.30(15)	1.160
LT4	X144-1	1307	21	1.317(3300)	3.104(298)	1.259(1209)	11.8	99.9	0.986	56.9±6.0	13.93±0.21(52)	1.550
LT5	X146-10B	2144	21	1.314(3293)	0.7721(105)	0.4882(664)	4.6	82.0	0.885	36.5±4.9	14.31±0.22(14)	0.000
LT6	X112-1	1940	9	1.320(3307)	2.217(102)	1.115(513)	10.4	3.8	0.918	41.6±7.9	14.40±1.26(2)	1.780
LT7	X111-1	2518	21	1.323(3314)	0.2512(27)	0.3284(353)	3.1	92.2	0.498	17.8±3.9	12.02±0.00(1)	0.000
LT8	X146-10C	2170	9	1.326(3321)	12.59(573)	3.024(1376)	28.1	0.000	0.988	49.3±14.8	14.90±0.22(30)	1.240
LT9	X142-2	1963	8	1.329(3328)	5.181(215)	1.655(687)	15.3	0.000	0.788	61.1±15.8	14.64±0.28(24)	1.410
LT10	X146-10S	2094	13	1.332(3335)	1.125(63)	0.5839(327)	5.4	11.1	0.944	45.1±7.3	12.70±0.52(12)	1.810
LT11	X140-4	2385	21	1.335(3342)	0.4331(68)	0.1573(247)	1.4	99.0	0.684	64.4±10.4	13.93±0.35(11)	0.830
LT12	X141-1	2030	4	1.341(3356)	2.069(60)	1.097(318)	10.1	9.5	0.985	44.4±7.3	11.91±0.52(4)	1.050
LT13	X143-2	1670	21	1.347(3370)	1.728(261)	0.7252(1095)	6.6	86.1	0.922	56.3±6.1	13.17±0.25(34)	1.470
LT14	X149-13	1572	9	1.350(3377)	13.53(582)	2.793(1201)	25.4	0.000	0.463	90.3±27.6	13.28±0.33(47)	2.300
LT15	X149-9	1840	3	1.816(4541)	4.950(99)	3.035(607)	20.6	0.630	1.000	27.6±14.7	14.69±0.25(3)	0.430
LT16	X149-8	2170	23	1.821(4552)	2.630(359)	2.320(3167)	15.7	91.6	0.965	36.3±3.6	13.41±0.22(40)	1.450
LT17	X149-2	1653	23	1.826(4563)	0.3187(42)	1.468(1935)	9.9	100.0	0.684	7.0±1.2	11.48±0.68(6)	1.680
LT18	X152-1	1540	23	1.830(4574)	0.1698(18)	0.6179(655)	4.2	98.7	0.470	8.9±2.2		
LT19	X152-6	1497	23	1.834(4585)	3.302(591)	1.159(2075)	7.8	90.1	0.960	91.4±8.8	13.54±0.18(40)	1.160
LT21	X136-1	1857	23	1.844(4607)	0.5600(49)	0.7543(660)	5.0	86.2	0.667	24.1±4.1	13.24±1.31(3)	2.280
LT22	X137-1	1650	8	1.848(4618)	0.6582(26)	1.096(433)	7.3	77.2	0.807	19.5±4.3	13.60±0.00(1)	0.000
LT23	151-1	1586	11	1.852(4629)	0.8293(34)	1.673(686)	11.1	64.3	0.995	16.2±3.1	12.65±0.57(3)	1.600
LT24	131-1	1955	22	1.857(4640)	2.305(204)	2.527(2236)	16.7	100.0	0.980	29.8±3.3	12.77±0.34(21)	1.570
LT25	134-4	2121	23	1.862(4651)	0.6606(72)	0.8560(933)	5.7	100.0	0.941	25.3±3.7	11.98±0.42(13)	1.520
ZrLT1	X146-10A	2094	6	0.3074(763)	15.08(193)	2.883(369)	115.4	0.000	0.300	27.2±6.9	±()	
ZrLT2	X147-1	1890	10	0.3076(764)	21.69(488)	3.213(723)	128.5	0.000	0.861	28.3±6.7	±()	
ZrLT3	X147-8	1890	10	0.3078(765)	67.02(1461)	5.234(1141)	209.2	0.000	0.798	63.9±9.5	±()	
ZrLT4	X144-1	1307	10	0.3080(766)	29.39(529)	2.406(433)	96.1	0.021	0.732	65.2±8.8	±()	
ZrLT6	X112-1	1940	5	0.3082(767)	92.17(1060)	5.870(675)	234.2	0.245	0.997	74.7±8.1	±()	
ZrLT11	X140-4	2385	10	0.3084(768)	58.49(1778)	3.266(993)	130.3	0.013	0.964	88.5±7.7	±()	
ZrLT12	X141-1	2030	7	0.3086(769)	66.76(1135)	3.924(667)	156.4	0.001	0.956	83.7±9.7	±()	
ZrLT20	X152-5	1540	10	0.3088(770)	83.83(2079)	5.685(1410)	226.5	0.001	0.943	81.7±6.9	±()	
ZrLT25	X134-4	2121	5	0.3090(771)	43.66(358)	3.280(269)	130.6	0.271	0.954	64.8±11.0	±()	

a) ρ_s, Spontaneous fission−track density; N_s, total number of fission tracks counted in s; ρ_i, induced fission-track density; N_i, total number of fission tracks counted in ρ_i; $P(x^2)$, probability where degrees of freedom=$(n^{-1})x^2$; n, number of samples for dating; r, correlation coefficient between N_s and N_i; T, age (mean age used when pooled data failed chi square test at 5%, the chi age used when pooled data succeeded chi square test at 5%); Standard glass is RM612, (Zeta=352.4±29). * The track lengths of the rest are undergoing calculation

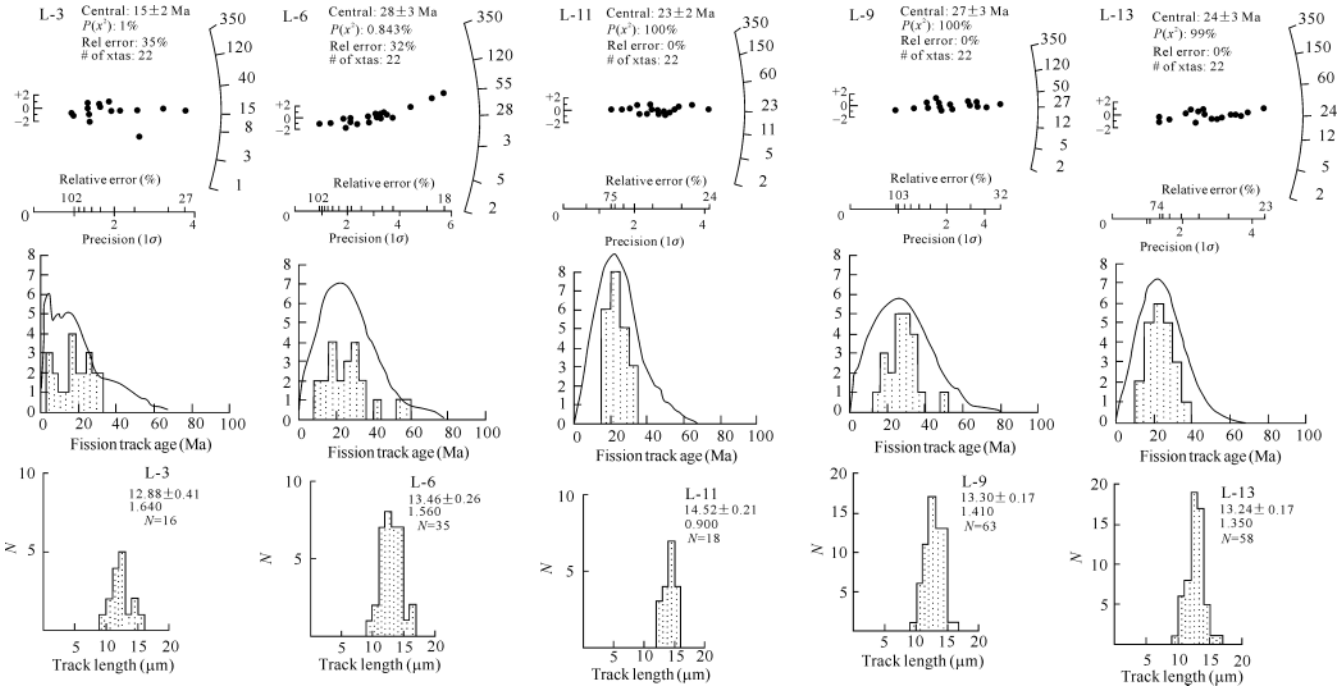

Figure 6 Length of apatite fission track and ages of Single apatite. The first and second lines are figures of ages, the third one is the figure of lengths.

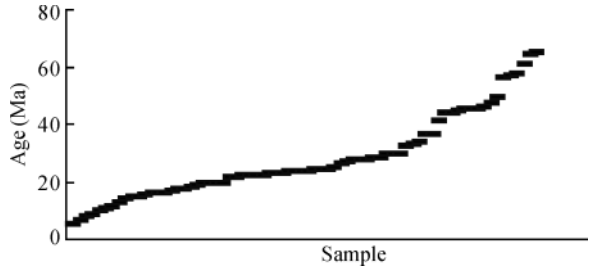

Figure 7 Distribution of Fission track ages of the Bogda-Balikun Mountain chain.

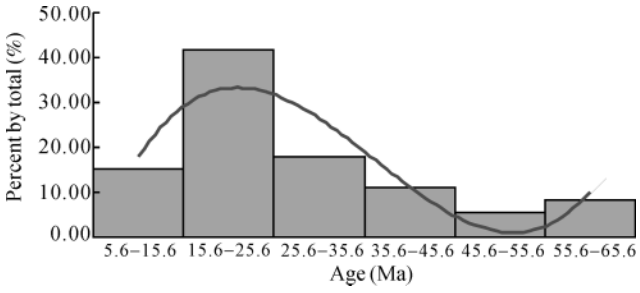

Figure 8 The histogram diagram of fission track ages of the Bogda Mountain and Balikun Mountain.

The distribution as a whole of these fission track ages of the studied region corresponded to the transformation of tectonic mechanisms of the eastern Xinjiang well. Under the setting of the Mesozoic extension, the eastern Xinjiang underwent pan-lake sedimentation in the Cretaceous, but closed gradually in Late Cretaceous, which mean that the depression in this time reached its maximum, and after this period, new tectonic mechanism developed. So the age of 65.6 Ma was the initial time of the regional inversion of the region.

6.2 Migration tendency of the uplifting

(1) Uplifting along the axis of the mountain. This study showed that there were obvious differences of uplifting time along the east–west direction of the mountain. The histogram of different segments of the mountain showed that there was an obvious jump of the uplifting age in the eastern Balikun Mountain during the Miocene (Figure 9(a)), and clocks of more than 50% of the samples were started at this time, which indicates more regions were involved into the uplifting process. This peak value is higher than those in the past, indicating that the uplifting of the Balikun Mountain was spasmodic.

Different from the Balikun Mountain, the uplifting of the Bogda Mountain to the west was much more gradual progressive (Figure 9(b)). Although the Miocene still held the peak value of the highest frequency, the difference from frequencies in the past was smaller, this is different from the Balikun Mountain.

In order to further study the differences of uplifting along the axis of the mountain, we sort the sampling

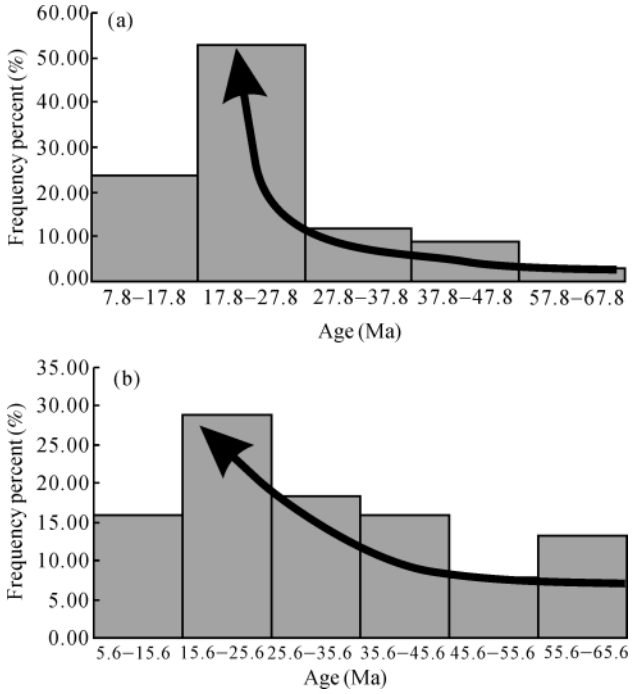

Figure 9 The distribution of fission track ages in east-west direction of Bogda-Balikun Mountain. (a) Balikun Mountain; (b) Bogda Mountain.

points based on their longitudes, and the distribution of fission track ages along the axis of the mountain was obtained (Figure 10). In Figure 10 the general migration tendency of mountain uplifting was showed by linear tendency line, and the eastern part was earlier than the western part; and cubic polynomial curve indicated that the migration of uplifting developed by complex way, and the uplifting of the Bogda Mountain started first at above 88.5°—89°E, and to the east and west of this point the uplifting became younger gradually. The tendency line shows arcute style: the fitted tendency age on the top of the arc is 45±5.0 Ma, the age of the west end is 15±1.5 Ma, and the age of the east end (91.5°E, i.e. Qijiaojing region) is 25±2.5 Ma. In contrast the age tendency line of the Balilun Mountain showed characteristics of younger in the middle and older at the two ends.

The general change of ages showed that the mountain is younger eastwards and older westwards, which is harmonious with the general tendency of the Cenozoic uplifting the Tianshan Mountains indicating that the Cenozoic uplifting of the Bogda-Balikun Mountain and the Western Tianshan Mountains was controlled by the same tectonic mechanism; the complex migration tendency of the uplifting showed by the cubic tendency line should be the exhibition of concrete tectonic events controlling the uplifting of the Bogda-Balikun Mountains, which were controlled by the tectonic segmentation and different deformation styles of various segments. The uplifting of the Balikun Mountain was the continuity of the Bogda Mountain.

(2) Differences in the south-north direction across the mountain. In order to understand the characteristics of the mountain uplifting and further to compare the uplifting ages of the north and south slopes of the mountain chain, we divide the sampling points into north group and south one taking the watershed of the mountain as the boundary. The Figure 11(a) showes the histogram of age distribution, in which abscissa axis is the number of samples, ordinate axis is age, the region to the left of the ordinate axis is the histogram of ages of the north slope, the right one is the histogram of ages of the south slope. The figure showed three points obviously: first, the initial uplifting age of the north slope were obviously earlier than those of the south slope; second, the whole mountain underwent uplifting for the time during 35—40 Ma; third, in the Miocene the age frequencies of both slopes were all up to their peaks, and the mountain underwent the main uplifting. Figure 11(b)

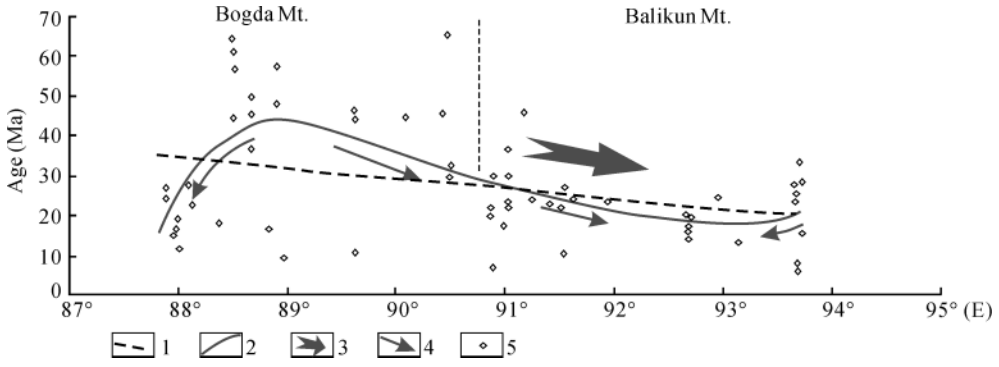

Figure 10 Uplifting migration of the Bogda-Balikun Mountain along the mountain axis. 1, Tendency line of age distribution (linear); 2, tendency line of age distribution (cubic polynomial curve); 3, general uplifting tendency; 4, subordinated uplifting tendency; 5, data points

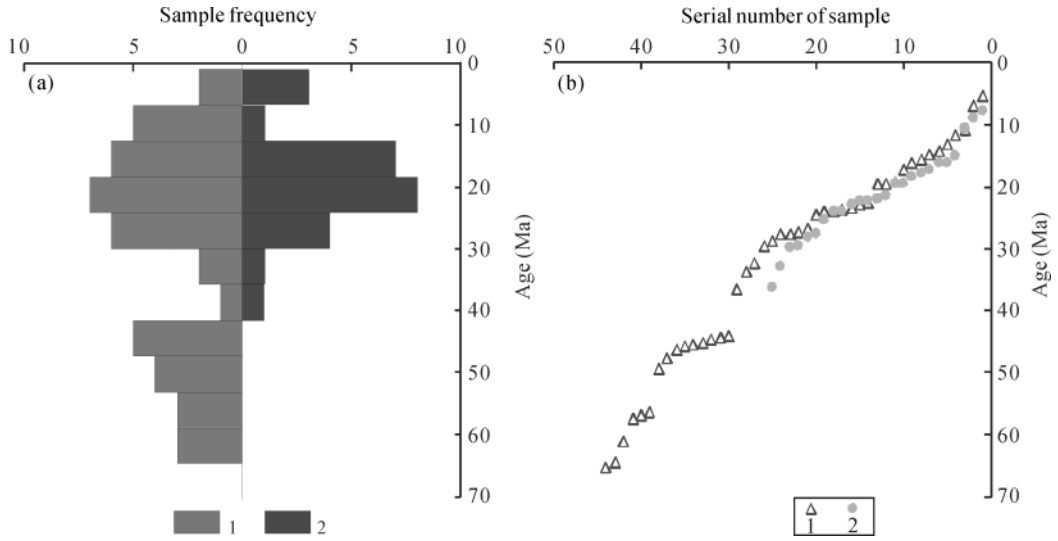

Figure 11 Distribution of fission track ages of south and north slopes of the Badga−Balikun Mountains. (a) Frequency of age distribution; (b) distribution of ages. 1, Data point to the north of watershed; 2, data point to the south of watershed.

is the distribution of the ages, the triangles are the ages of the north slope, and the circle points show the ages of the south slope The distribution of these two age groups also showed the uplifting difference between two slopes, i.e. early in the north and late in the south. As mentioned earlier, the points of initial uplifting of the Bogda Mountain are distributed mainly in the western part (Figure 10), and furthermore, geophysical data showed that the Junggar Basin is underthrust beneath the western part of the Bogda Mountain. However, no such phenomenon occurred eastwards (including the Balikun Mountain), and therefore the Cenozoic uplifting may have occurred in the western part first, with the continuous underthrusting of crust to the north, while the uplifting developed eastwards and southwards.

(3) Uplifting rate best-fit line and pattern. In addition to the division of fission track ages with the watershed as the boundary, the length distribution of apatite fission tracks of the two groups was also calculated. The lengths of tracks range from 10.72−14.92 μm. A total of 875 fission tracks from the north slope and 466 from the south slope were used. Based on these data, the histogram of length distribution was obtained (Figure 12). The Figure 12 showed two characteristics of length distribution First, single peak distribution is the main pattern of the two groups, and the peak of the north slope is L_{max}=13.5−14.2 μm and that of the south slope is L_{max}=12.8−13.5 μm, which are all the standard type of heating history of non-disturbance basement All these mean that the mountain as a whole has not been buried

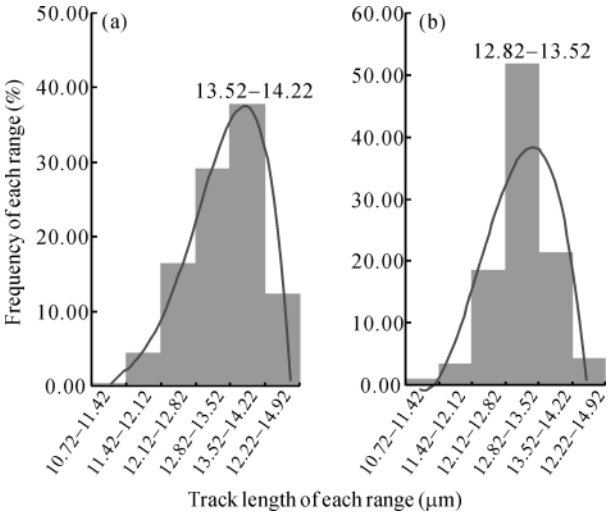

Figure 12 Distribution of AFT length across the mountain. 1, Data points to the north; 2, data point to the south.

deeply or undergone other heating events after the beginning of uplifting. Second, the measured lengths of fission tracks were obviously shorter than the lengths of typical induced fission tracks, which indicates the annealing of the fission tracks of the mountain had occurred, i.e. samples did not become denudated to the surface rapidly and directly after they entered into the close temperature, but stayed for some time in the annealing zone.

In order to better discuss the uplifting rate of mountain, we selected 30 samples of apatite and used AFT-solve software to make fit calculations of fission track length with age, and put all best-fit lines together to ob-

tain the fit curves of Cenozoic uplifting rate of orogenic belt to the south of eastern Junggar Basin (Figures 13 and 14). Modeling results show that: 1) the beginning time of uplifting of the orogenic belt mainly ranged from 60 Ma to 70 Ma, and the main uplifting occurred in the Miocene from 15 Ma to 27 Ma; 2) although most curves show the state of orogenic belt's uplifting, there is no unchangeable velocity by which the mountain uplifted, contrarily all curves show that the uplifting stopped sometime in the whole process of uplifting The temperature range for the ceasing is 50—70℃, and at last during the Later Pleistocene about 5—3 Ma, when the second rapid uplifting has begun; 3) some samples also show that there was a secondary slow uplifting during 70—50 Ma.

7 Discussion on dynamics of uplifting

It is well known that the collision and consequently convergence between the Indian and Eurasian plates resulted in not only the reverse of the Mesozoic structures in the Tianshan Mountains and the re-uplifting of Tianshan Mountains, but also the terrestrial clastic deposition in foreland basins to the south and north of mountain, and the formation of present basin-range pattern[9,20]. However, crucial problems are how the compressive stress produced along the plate boundary can be transferred to the Tianshan Mountains, and how the stress resulted in the deformation of Tianshan Mountains. This study showed that the initial uplifting of the Bogda-Balikun Mountains began at ca. 65 Ma; however was this uplifting the effect of the beginning collision between the Indian–Eurasian Plates? Many recent studies have showed that the Indo–Eurasian collision took place between 65—45 Ma[21,22]. In addition, Chen et al.[23] and Avouac et al.[24] pointed out that the main reason for the deformation of the Tianshan Mountains and crustal shortening was the clockwise rotation of the Tarim block about 9° based on the paleogeomagnetic mode. Deng et al[4] proposed that the distance of the Tianshan Mountains to present collisional boundary is about 2000km, and the shortening and convergence was absorbed by the crustal thickening of the Qinghai-Tibet Plateau[25], rotating of interior blocks of plateau[26,27], and eastward extrusion of blocks[4,24,28–30] And some other studies argued the Indo-Eurasian collision also affect the Tianshan Mountains, or even Mongolia[16]. Our results show that the Eastern Tianshan Mountains undertook slow uplifting during 65—35 Ma (Figures 12 and 13), which may mean that the effect of the Indo-Eurasian collision may have touched the Eastern Tianshan Mountains at that time, but it was very weak. Although without more data, we incline that the initial slow uplifting of the Eastern Tianshan Mountains during the Early Cenozoic did not result from the Indo-Eurasian collision, and instead the tectonic function of the Siberian plate should be considered. Many studies have shown that the period of 17—23 Ma is one of main stages of uplifting of the Qinghai-Tibet Plateau[1,2,31—40],

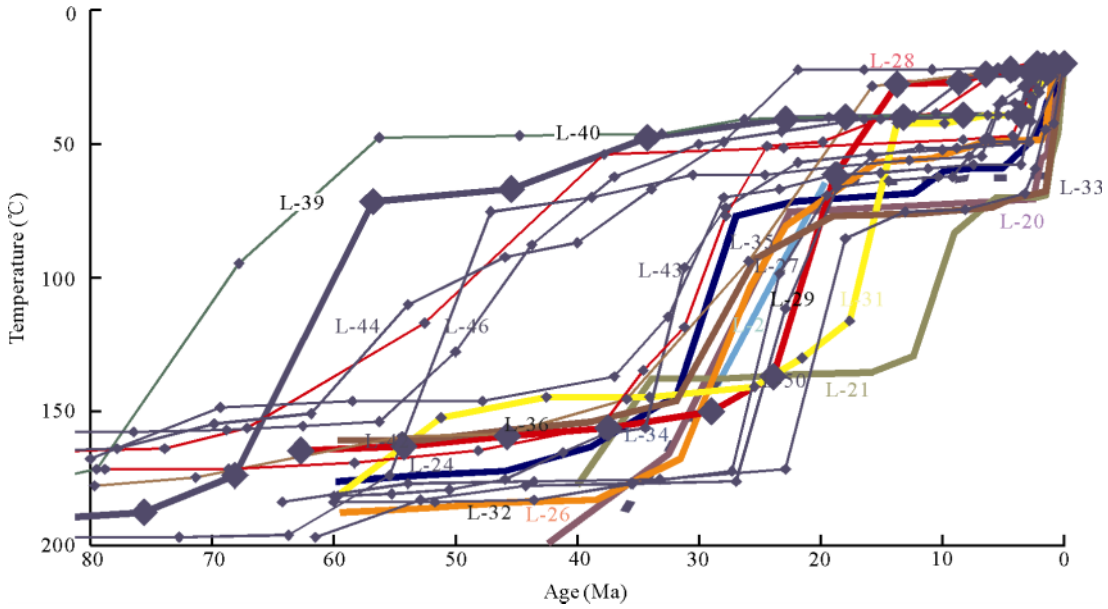

Figure 13 AFT fission track length-ages best-fit line of the Bogda-Balikun Mountains.

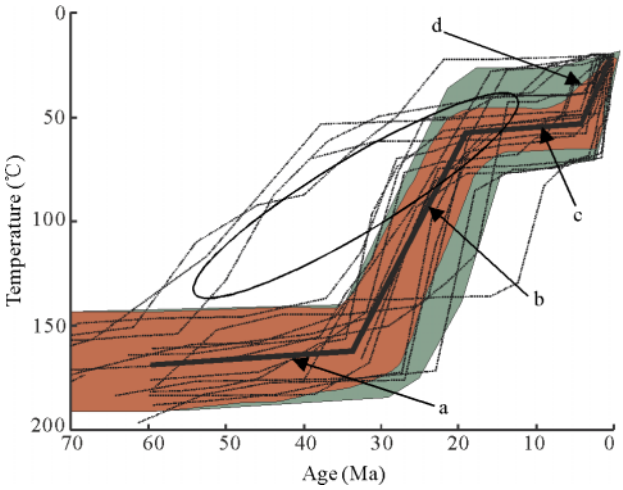

Figure 14 AFT uplifting rate pattern of the Bagda-Balikun Mountains. (a) Initial uplifting; (b) rapid uplifting at above the Miocene; (c) detained annealing; (d) rapid uplifting.

and it not only was one important period for tectonic transformation from early large scale strike-slipping to late crust thickening[41,42] but also one important period for the Plateau to expand to the north[43−46]. This study showed the strong uplifting of Eastern Tianshan Mountains also occurred in about 24 Ma, so we suggest that the uplifting of the whole Tianshan Mountains during Oligocene-Miocene has a close relation to the coeval tectonic events of the Qinghai-Tibet Plateau, which was the response of the northward expanding of the Plateau. Moreover, the Qinghai-Tibetan Plateau has undertaken another rapid uplifting and deformation in the Late Cenozoic[47−55], and this tectonic event was also recorded in the Eastern Tianshan Mountains. Although we still could not affirm whether the Cenozoic uplifting of the Eastern Tianshan Mountains has direct relationship with the Indo-Eurasian collision or not, the above analysis showed that the uplifting of the Tianshan Mountains in the Cenozoic has much closer relationship with the evolution of the Qinghai-Tibet Plateau, especially with those tectonic events occurred in the northern plateau.

8 Conclusions

(1) The initial uplifting of the Bogda Mountain and the Balikun Mountain was no later than the Paleocene (65 Ma). During the Eocene to the Oligocene, the mountain underwent one prevalent uplifting, although the mainly uplifting of this mountain chain occurred about 24.4 Ma in the Miocene. From 20 Ma to 5.6 Ma, the mountain underwent uneven and differential uplifting. The initial uplifting at 65 Ma probably was the startup time of re-orogeny of the Bogda Mountain, which is consistent with the time restricted by re-construction of foreland basins in the north and south of mountain[1)], and is 40 Ma earlier than the startup time (24 Ma) of re-orogeny proposed by Hendrix et al.[1] and Deng et al.[4].

(2) The prominent character of re-orogeny in the Cenozoic is the differential uplifting of the mountain chain along the EW and NS direction. The cooling ages become younger from west to east gradually. Three stages of uplifting can be found in Bogda Mountain and the later two stages occurred in the Balikun Mountain, and the uplifting of the conjunction between the Bogda Mountain and Balikun Mountain (Qijiaojing) took placed during the second stage. Along the south-north direction, the north slope of the eastern Bogda Mountain may uplift earlier and extend to the south gradually.

(3) The fission track age with track length above 14 μm (including 14 μm) concentrates on about 24 Ma, suggesting the uplifting in the Miocene is rapid. The results also show that the uplifting rate becomes higher as the age gets younger. However, the age with fission-track length of 13.61 μm is 65.3 Ma, indicating that the uplifting rate of the first stage is slower than that of the second stage when the mountain body went through the annealing zone.

(4) Of three tectonic events, two of the Bogda-Balikun Mountains uplifting in the Cenozoic could compare with those events occurred in the northern part of the Qinghai-Tibet Plateau in the Cenozoic (5.6−19 Ma, 20−30 Ma), and thus the uplifting of the Eastern Tianshan Mountains since the Miocene may be the response of the evolution of the northern part of the Qinghai-Tibet Plateau. And the slow uplifting of the Mountain at the end of the Mesozoic may have close relationship with the Siberian plate.

We thank Wan Jinglin of Institute of Geology, China Seismological Administration who carried out the measurements of fission track. We also thank Prof. He Guoqi sincerely for his constructive suggestions. We heartily thank Ms. Yan Xili for making the computer graphics.

1) Wang Z X. Orogeny, Formation and evolution of Bogad Mountain, Northwest China. Doctor Dissertation. Beijing: Institute of Geology, China Seismological Administration, 2003.30−55

1 Hendrix M S, Dumitru T A, Graham S A. Late Oligocene–early Miocene unroofing in the Chinese Tianshan: An early effect of the India-Asia collision. Geology, 1994, 2: 487－490
2 Sobel E R, Trevor A D. Thrusting and exhumation around the margins of the western Tarim Basin during the India-Asia collision. J Geophys Res, 1997, 102 (B3): 5043－5063
3 Shu L S, Wang B, Yang F, et al. Polyphase tectonic events and Cenozoic basin–range coupling in the Tianshan belt, northwestern China. Acta Geol Sin, 2003, 77 (4): 457－467
4 Deng Q D, Feng X Y, Zhang P Z, et al. The Teotectonics of Tianshan (in Chinese). Beijing: Seismological Press, 2000. 36－248
5 Zhao J M, Liu G D, Lu Z X, et al. Lithospheric structure and dynamic processes of the Tianshan orogenic belt and the Junggar Basin. Tectonophysics, 2003, 376(3–4): 199－239
6 Yang G, Qian X L. Mesozoic–Cenozoic uplift of the Tianshan intraplate orogenic belt evidence from zircon and apatite fission track dating. Acta Scientiarum Naturalium Universitatis Pekinensis (in Chinese), 1995, 31(4): 473－478
7 Wang Y B, Wang Y, Liu X, et al. Apatite fission–track records of Mesozoic and Cenozoic episodic reactivation of the Tianshan and west Kunlun Mountains. Reg Geol China (in Chinese), 2001, 20(1): 94－99
8 Zhou Y Z, Chen H L. The fission track evidence of the uplift in Late–Cretaceous in the Kuche basin, Xinjiang. Volcanol Min Resour (in Chinese), 2002, 23: 179－184
9 Gong H L, Chen Z L, Hu Y Q, et al. Cretaceous denudation of the Ili basin as revealed by fission track thermochronology. J Geomech, 2007, 13(1): 42－50
10 Windley B F, Allen M B, Zhang C, et al. Paleozeoic accretion and Cenozoic rederofrmation of the Chinese Tian Shan Range, central Asia. Geology, 1990, 18: 128－131
11 Allen M B, Zhang C, Guo J H. Evolution of the Turpan basin, Chinese Central Asia. Tectonics, 1990, 12: 889－896
12 Ma R S, Shu L S, Sun J Q. Tectonic Evolution and Metallogeny of Eastern Tianshan Mountainss (in Chinese). Beijing: Geological Publishing House, 1997. 1－202
13 Shu L S, Lu H F, Yin D H, et al. Late paleozoic continental accretionary tectonics in northern Xinjiang. Xinjiang Geol (in Chinese), 2001, (1): 62－66
14 Xiao X C, Tang Y Q, Feng Y M. The Tectonics of the Northern Xingjiang and Its Adjacent Regions (in Chinese). Beijing: Geological Publishing House, 1992. 1－169
15 Wang Z X, Li T, Zhou G Z. Geological record of the late Carboniferous orogeny in Bogda mountain, northern Tianshan Mountains, northwest China. Earth Sci Front (in Chinese), 2003, 10(1): 63－69
16 Cunningham W D, Windley B F, Dorjnamjaa D, et al. Geometry and style of partitioned deformation within a late Cenozoic transpressional zone in the eastern Gobi Altai mountains, Mongolia. Tectonophysics, 1997, 277: 285－306
17 Liu Y Q, Wang Z X, Jin X C, et al. Evolution, chronology and depositional effect of uplifting in the eastern sector of the Tianshan Mountainss. Acta Geol Sin, 2004, 78(3): 32－44
18 Gleadow A J W, Duddy I R, Green P F, et al. Confined fission track lengths in apatite: A diagnostic tool for thermal history analysis. Contrib Mineral Petrol, 1986, 94: 405－415
19 Hurford A J, Green P F. A users' guide to fission track dating calibration. Earth Planet Sci Lett, 1982, 59(2): 343－354
20 Tapponnier P, Molnar P. Active faulting and tectonics in China. J Geophys Res, 1977, 82: 2905－2930
21 Yin A, Harrison T M. Geologic evolution of the Himalayan–Tibetan orogen. Annu Rev Earth Planet Sci, 2000, 28: 211－280
22 Molnar P, England P, Martinod J. Mantle dynamics, uplift of the Tibetan plateau, and the Indian monsoon. Rev Geophys, 1993, 31: 357－396
23 Chen Y, Cogne J P, Courtillot V, et al. Paleomagnetic study of Mesozoic continental sediments along the northern Tianshan and heterogeneous strain in central Asia. J Geophys Res, 1990, 96: 4065－4082
24 Avouac J P, Tapponier P, Bai M, et al. Active thrusting and folding along the northern Tian Shan and late Cenozoic rotation of the Tarim relative to Dzungaria and Kazakhstan. J Geophys Res, 1993, 98: 6755－6804
25 England P C, Houseman G A. Inite strain calculations of continental deformation 2, Comparison with the India-Asia collision zone. J Geophys Res, 1986, 91: 3664–3676
26 England P C, Molnar P. Right-lateral shear and rotation as the explanation for strike-slip faulting in eastern Tibet. Nature, 1990, 344: 140－142
27 Molnar P, Lyon-Caen H. Fault plane solution of earthquakes and active tectonics of the Tibetan Plateau and its margins. Geophys J Int, 1989, 99: 123－153
28 Tapponnier P, Pelzer G, Le D A Y, et al. Propagating extrusion tectonics in Asia: New insight from simple experiments with plasticine. Geology, 1982, 10: 611－616
29 Peltzer G, Tapponnier P. Ormation and evaluation of strike-slip faults, rifts, and basins during the India-Asia collision: An experimental approach. J Geophys Res, 1987, 93: 15085－15117
30 Xu X.W, Deng Q D. Nonlinear characteristics of paleoseismisity in China. J Geophys Res, 1996, 101(B3): 6209－6231
31 Tapponnier P, Lacassin R, Leloup P H, et al. The Ailao Shan/Red river metamorphic belt:Tertiary left-lateral shear between Indochina and South China. Nature, 1990, 343: 431－437
32 Hodges K V, Parrish R R, Housh T B, et al. Simultaneous Miocene extension and shortening in the Himalayan orogen. Science, 1992, 258: 1466－1470
33 Copeland P, Harrison T M, Kidd W S F, et al. Rapid early Miocene acceleration of uplift in the Gangdese belt, Xizang (south Tibet), and its bearing on accommodation mechanisms of the India–Asia collision. Earth Planet Sci Lett, 1987, 86: 240－252
34 Copeland P, Harrison T M. Eposodic rapid uplift in the Himalaya revealed by $^{40}Ar/^{39}Ar$ analysis of detrital K-feldspar and muscovite, Bengal Fan. Geology, 1990, 18: 354－357
35 Richer R M, Lovera O M, Harrison M, et al. Tibetan tectonics from $^{40}Ar/^{39}Ar$ analysis of a single K-feldspar sample. Earth Planet Sci Lett, 1991, 105: 85－92
36 Corrigan J D, Crowley K D. Unroofing of the Himalayas: review from apatite fission–track analysis of Bengal Fan sediments. Geophys Res Lett, 1992, 19: 2345－2348
37 Zeitler P K. Cooling history of the NW Himalaya, Pakistan. Tectonics, 1985, 4: 127－151

38 Treloar P J, Rex D C, Williams M P. The role of erosion and extension Pakistan Himalaya. Geol Mag, 1991, 128: 465－478
39 Cerveny P F, Naeser N D, Zeitler P K, et al. History of uplift and relief of the Himalaya during the past 18 million years: Evidence from fission–track ages of detrital zircons from sandstones of the Siwalik Group. In: Kleinspehn K L, Paolo C, eds. New Perspectives in Basin Analysis. New York: Springer-Verlag, 1988. 43－61
40 Downing K F, Lindsay E H, Downs W R, et al. Lithostratigraphy and vertebrate biostratigraphy and vertebrate biostratigraphy of the early Miocene Himalayan foreland, Zinda Pir Dome, Pakistan. Sediment Geol, 1993, 87: 25－37
41 Yue Y J, Liou J G. Two–stage evolution model for the Altyn Tagh fault, China. Geology, 1999, 27: 227－230
42 Yue Y J, Ritts B D, Graham S A. Initiation and long–term slip history of the Altyn Tagh fault. Int Geol Rev, 2001, 43: 1087－1093
43 Fang X, Carmala G, Van der V R, et al. Flexural subsidence by 29 Ma on the NE edge of Tibet from the magnetostratigraphy of Linxia Basin, China. Earth Planet Sci Lett, 2003, 210: 545－560
44 Zhang J, Ma Z J, Xiao W X, et al. Geological evidences of the deformation in central–southern Ningxia in the Miocene and its significance. Acta Geol Sin (in Chinese), 2006, 80(11): 1650－1659
45 Guo Z J, Zhang Z C, Wu C D, et al. The Mesozoic and Cenozoic exhumation history of Tianshan and comparative studies to the Junggar and Altai mountains. Acta Geol Sin (in Chinese), 2006, 80(1): 1－15
46 Du Z L, Wang Q C. Mesozoic and Cenozoic uplifting history of the Tianshan region: Insight from apatite fission track. Acta Geol Sin (in Chinese), 2007, 81(8): 1081－1101
47 Li J J, Wen S X, Zhang Q S, et al. Discussion on the age, amplitude and form of the uplifting of the Qinghai–Tibetan plateau. Sci China Ser A, 1979, (1): 88－102
48 Li J J, Fang X M, Ma H Z, et al. Geomorphological and environmental evolution in the upper reaches of the Yellow river during the late Cenozoic. Sci China Ser D-Earth Sci (in Chinese), 1996, 39(4): 380－390
49 Zheng H B, Powell C M, An Z S, et al. Pliocene uplift of the northern Tibetan plateau. Geology, 2000, 28(8): 715－718
50 Zhang P Z, Burchfiel B C, Molnar P, et al. Amount and style of late Cenozoic deformation in the Liupanshan area, Ningxia autonomous region, China. Tectonics, 1991, 10: 1111－1129
51 Burchfiel B C, Zhang P, Wang Y, et al. Geology of the Haiyuan fault zone, Ningxia–Hui autonomous region, China, and its relation to the evolution of the northeastern margin of the Tibetan plateau. Tectonics, 1991, 10: 1091－1110
52 Fang X, Yan M, Rob V, et al. Late Cenozoic deformation and uplift of the NE Tibetan plateau: Evidence from high-resolution magnetostratigraphy of the Guide Basin, Qinghai province, China. GSA Bull, 2005, 117(9-10): 1208－1225
53 Sun J M, Zhu R X, An Z S. Tectonic uplift in the northern Tibetan plateau since 13.7 Ma ago inferred from molasse deposits along the Altyn Tagh fault. Earth Planet Sci Lett, 2005, 235: 641－653
54 Fang X M, Song C H, Dai S. Cenozoic deformation and uplift of the NE Qinghai–Tibet plateau: Evidence from high–resolution magnetostratigraphy and basin evolution. Earth Sci Front (in Chinese), 2007, 14(1): 230－242
55 Li S J. Latitudinal convergence of the Asian continent, rise of the Qinghai Tibet Plateau and expansion of the east Asian continent. J Geomech, 2007, 13(1): 25－30